Veterans' Glass City Skyway Bridge Main Cable Evaluation

Prepared by:
Serhan Guner

Prepared for:
The Ohio Department of Transportation,
Office of Statewide Planning & Research

Project ID Number: *118075*

May 2025

Final Report

THE UNIVERSITY OF TOLEDO
Department of Civil and Environmental Engineering

OHIO DEPARTMENT OF TRANSPORTATION
RESEARCH

U.S. Department of Transportation
Federal Highway Administration

Technical Report Documentation Page

1. Report No.	2. Government Accession No.	3. Recipient's Catalog No.

4. Title and Subtitle	5. Report Date
Veterans' Glass City Skyway Bridge Main Cable Evaluation	**May 2025**
	6. Performing Organization Code

7. Author	8. Performing Organization Report No.
Serhan Guner	

9. Performing Organization Name and Address	10. Work Unit No. (TRAIS)
The University of Toledo **2801 W. Bancroft** **Toledo, Ohio 43606-3390**	
	11. Contract or Grant No.
	PID: 118075

12. Sponsoring Agency Name and Address	13. Type of Report and Period Covered
Ohio Department of Transportation **1980 West Broad Street** **Columbus, Ohio 43223**	**Final Report**
	14. Sponsoring Agency Code

15. Supplementary Notes

16. Abstract

The most critical and prevalent condition causing cable deterioration is the corrosion of the steel strands inside the stays. Stay cables of the Veterans' Glass City Skyway (VGCS) have unique design features to help reduce and delay strand deterioration. These features also make it difficult to inspect the strands using currently available non-destructive evaluation (NDE) methods. The objective of this study is to identify practical nondestructive methods for monitoring and assessing the condition of the strands of the VGCS using existing technologies and develop a long-term monitoring and assessment plan.

Literature searches, case studies, and subject-matter expert interviews indicate that the deterioration of strands typically starts at the anchorage zones. The applicable methods for the inspection of these zones include visual inspection methods, and material sampling and testing. The applicable methods for global health assessment include the vibration-based cable tension estimation methods. The applicable methods for the free lengths of the strands include magnetic flux leakage (MFL) testing using a custom-designed magnet or pulling and replacing a few selected strands and testing them in a laboratory.

The visual inspection study conducted using a borescope inspected the lower ends of 14 stays, and found no evidence of strand damage, chipping, or corrosion. The dusty state of the strands implies no water runoff and dry conditions. The grease samples collected from the lower ends of the stays appeared in good condition with consistent color, viscosity, and consistency. The environmental condition assessment study performed using six internal and two external temperature and humidity loggers found no evidence of excessive moisture accumulation inside the stays. The stay force estimation study conducted using a laser vibrometer on 20 stays found no credible concern for the health of the stay cables of the VGCS.

As a part of a long-term monitoring and assessment plan, this study recommends establishing a periodical cable tension estimation program with a 4-year cycle, and applying the NDE methods recommended in this report as a part of a regular inspection program. If evidence of notable strand deterioration is detected, the two NDE methods identified in this report should be considered for the free lengths of the strands.

17. Keywords	18. Distribution Statement
Borescope inspection, cable tension estimate, dew point, humidity, laser vibrometer, magnetic flux leakage, non-destructive testing, stay cables, strand deterioration, strand corrosion, temperature.	**No restrictions. This document is available to the public through the National Technical Information Service, Springfield, Virginia 22161**

19. Security Classification (of this report)	20. Security Classification (of this page)	21. No. of Pages	22. Price
Unclassified	**Unclassified**	**40**	

Form DOT F 1700.7 (8-72) **Reproduction of completed pages authorized**

Veterans' Glass City Skyway Bridge Main Cable Evaluation

Prepared by

Serhan Guner

Department of Civil and Environmental Engineering
The University of Toledo
Toledo, Ohio 43606-3390

Prepared in cooperation with the Ohio Department of Transportation
and the U.S. Department of Transportation, Federal Highway Administration

Final Report
May 2025

Acknowledgments

The author would like to thank the Ohio Department of Transportation (ODOT) for funding and supporting this research. The author is grateful to the ODOT Technical Advisory Committee members Mr. David Geckle, P.E., and Mr. Jared Backs, P.E., for their time, support and feedback, and to ODOT Program administrators Ms. Jill Martindale and Ms. Jennifer Spriggs for managing the project and arranging monthly meetings. The author is grateful to Dr. Douglas Nims, Dr. Daniel Georgiev, and MS students Suraj Dhungel, Sandeep Bajagain, Yugesh Maharjan, and Prativa Pathak for their help with the project. The Department of Civil and Environmental Engineering at the University of Toledo is also acknowledged for providing the facilities needed for this research.

Table of Contents

List of Figures

List of Tables

1. Problem Statement

Stay cables are the most vulnerable component of cable-stayed bridges. The most critical and prevalent condition causing cable deterioration is the corrosion of the steel strands inside the stays. Other types of deterioration conditions include section loss, pitting, breakage or nicking, compromised grout or grease, voids, and water infiltration.

The Veterans' Glass City Skyway (VGCS) was opened to traffic in 2007. It is important to have a non-destructive evaluation (NDE) strategy in place to monitor the conditions of the stay cables. This could enable timely remedial actions if/when strand deterioration is detected. The VGCS stays are unique. The strands in each stay are epoxy-coated and encased within a stainless-steel sheathing (Figure 1a). The sheathing is large, and the strands are non-compacted with no filler or grout used. Cheese plates at certain locations provide separation of the strands (Figure 1b). For the longer stays, the strands are able to vibrate inside the stays, hitting each other and sheathing. This may cause deterioration in the epoxy coating over time. In addition, epoxy coating is susceptible to localized peeling during installation.

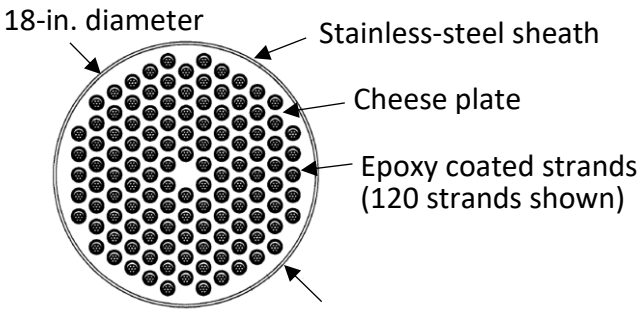

(a) Strands at the cheese plate

(b) Cheese plate

Figure 1 Non-compacted and non-grouted stays of the VGCS.

Typical stays commonly used in other bridges are smaller, made of high-density polyethylene, and the void space is filled with a filler such as grout (Figure 2 [1]). The ongoing NDE stay inspection practice and research are focused on filled stays. There is a lack of research and knowledge on the corrosion susceptibility and NDE methods applicable to the type of sheath-strand configuration used in the VGCS.

Figure 2 Grout-filled stays used commonly on other bridges.

2. Objectives of the Study

The objective of this study is to identify practical nondestructive methods for monitoring and assessing the condition of the strands of the VGCS using existing technologies and develop a long-term monitoring and assessment plan.

3. Research Background

The design of the VGCS has unique components to help reduce and delay strand deterioration. They include:

- The epoxy-coated strands with filled interstices (Figure 3). Past research shows excellent performance of this type of strand for corrosion protection. However, the nicking of or damage to the coating (e.g., during installation or due to inter-strand contact) can lead to peeling of the coating, exposing the bare strands [2].
- The stainless-steel cable sheathing serves as the first line of defense barrier against damage or intrusion of harmful substances from the outside. The large diameter of the sheathing, however, makes most current NDE methods inapplicable.
- Ungrouted strands that allow for the replacement and inspection of a single strand. The extracted strand(s) can be tested in a laboratory to assess their condition.
- A cradle system in which each strand passes through its own stainless-steel sleeve within the cradle assembly. This reduces inter-strand contact and associated deterioration (e.g., fretting and fatigue).

These features also make it difficult to inspect the strands using currently available non-destructive evaluation (NDE) methods.

(a) Label and date stamp *(b) Cross section of the strand sample*

Figure 3 VGCS strand sample from the construction.

The most common condition causing cable deterioration is the corrosion of the steel strands. Corrosion is an electrochemical process that can negatively affect the strength or service life of any metal element. The mechanism of strand corrosion is complex, and the factors leading to corrosion are highly random in nature [3]. It is well documented that moisture and oxygen are required for the corrosion process to occur in addition to the transfer of an electric charge in an aqueous solution. Other factors that can affect the rate or type of corrosion include temperature, wind, airborne contaminants, alloy content, biological organisms, and others [4]. Depending on these factors, different types of corrosion may take place, including uniform corrosion,

atmospheric corrosion, chloride-induced corrosion, carbon dioxide concentration, pitting corrosion, corrosion cracking, fretting fatigue, galvanic corrosion, and hydrogen-induced stress corrosion [2]. Consequently, it is important to monitor the environmental conditions inside the stays of the VGCS and assess whether the conditions are conducive to corrosion.

Corrosion can cause many types of premature failure of strands. The first type of failure that can occur is a brittle failure due to corrosion pitting, in which localized corrosion notches the strand, reducing its ability to hold the required load. Second, a common phenomenon called hydrogen-induced stress corrosion cracking occurs when a crack forms and propagates under the influence of a corrosive environment and tensile stresses. This method of failure can occur without visible corrosion product, making it particularly difficult to detect [5]. Fatigue tests on parallel wire cables have shown that the yield and ultimate strengths of the strands are somewhat unaffected by uniform corrosion, but their ductility greatly decreased, and the variability in mechanical properties increased significantly [6]. Similarly, the fatigue life of corroded strands is significantly less than non-corroded wires, as corrosion speeds up fatigue crack propagation and ultimate fatigue fracture of the strands [6].

The relevant literature, case studies, and subject matter expert interviews conducted for this study indicate that the deterioration of strands typically starts *at the anchorage zones* as opposed to the free lengths of the strands (Figure 4 [1,7]). Factors contributing to this phenomenon at the anchorage zones include high-stress concentrations, high potential for water ponding, exposure to de-icing chemicals and other contaminants, large transverse forces in the saddles especially at the entrances to the pylon, and the deterioration of water infiltration prevention measures over time (e.g., washers, rings, filler grease, etc.).

(a) Significant corrosion found in an anchorage *(b) Water exiting the end cap of the anchorage*

Figure 4 Sample corrosion cases at the anchorage zones.

Fortunately, inspection of anchorage zones is simpler for the VGCS than that of free lengths of strands. The available methods include removal of anchorage caps and sleeves access at the deck; visual inspection of strand ends, sockets, and locking plates; visual inspection of difficult-access locations such as anchorage boxes and guide pipes using borescopes; dissection of sheathing for visual inspection of fillers and strands; and material sampling and testing [1].

Non-destructive inspection of the free lengths of strands requires more advanced methods, which may include magnetic flux leakage (MFL), MFL-magnet, magnetic main flux method (MMFM)-solenoid, and electrochemical impedance spectroscopy (EIS). The accuracy of these methods in detecting corrosion may range from moderate to high [2] for cases involving 5 and 10% section loss, respectively.

4. Research Approach

The research approach includes the following:

- Conduct a literature search on the published studies and project reports.
- Reach out to firms providing NDE services and experts in the national committees on NDE.
- Identify a collection of NDE methods that are applicable to the VGCS stays.
- Evaluate the effectiveness, reliability, and site-deployment characteristics of each method.
- Identify candidate vendors and the estimated costs for the applicable methods.
- Use the most suitable methods to assess the current condition of the VGCS stays.
- Develop a long-term monitoring and assessment plan.

The research results implementation approach includes evaluating the condition of high-risk but easier to inspect areas first (e.g., anchorage zones), and if evidence of notable strand deterioration is detected, considering the evaluation methods for lower-risk and more difficult to inspect areas (e.g., free lengths of the strands).

The NDE methods applied in this study include the visual inspection of the lower ends of the stays above the anchorage zone, environmental condition monitoring inside the stays, and stay force estimation and comparison with healthy values as a global health assessment.

The following sections present the identified NDE methods applicable to VGCS and the studies undertaken in applying them.

4.1. Visual Methods

Visual testing methods are extensively used for the inspection of hard-to-reach areas. The studies indicate the suitability of a borescope inspection of the lower ends of the stays above the grease line. The available drain holes can serve as the required access ports (Figure 5). This requires selecting a suitable borescope with a probe small enough to fit the existing holes. The lower ends of the stays are a high-risk location for corrosion and other types of deterioration conditions. Therefore, such an inspection can give valuable information about the condition of the lower ends of stay cables. A borescope inspection can also help assess the condition of the grease (e.g., viscosity, level, and presence of ridges). This method provides capabilities for taking photos and videos as needed during the inspection. Due to the visual nature of the method, its accuracy and reliability are high.

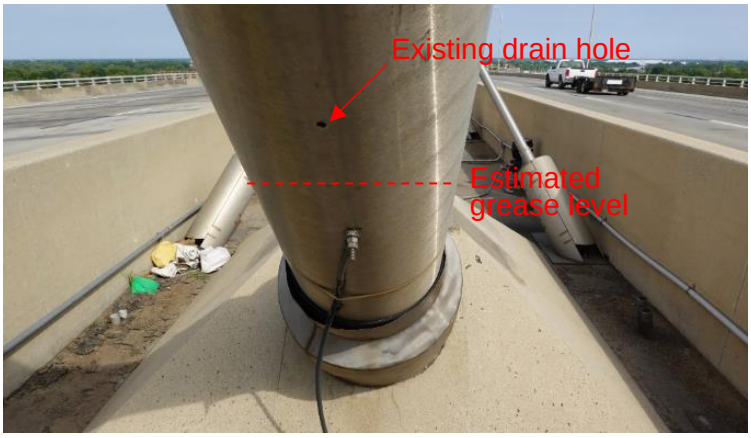

Figure 5 Lower ends of stays with a drain hole.

For the VGCS, the research found the dual camera borescopes to be the most suited among various options (Figure 6). These units have a side-view camera in addition to the traditional front-view camera. This can allow better inspection of the strands when the probe is inserted parallel to the strands. A four-way articulation capability is also needed. This uses a manual or electronic mechanism via a user-controlled joystick to move the probe in all four directions. This allows more precise movement of the probe towards the areas of concern during an inspection. Almost all current borescopes are powered by rechargeable batteries with an average service life of three hours. Consequently, multiple battery packs are required for an inspection which may take the entire day.

Figure 6 Sample borescope with a dual-view camera.

Another important consideration is the capability for inspecting areas above the probe insertion point. Borescopes use gravitational forces for the advancement of the probe and are typically used to inspect areas lower than the probe insertion port. For the

VGCS stays, it is important to inspect the strands above the insertion hole (Figure 5) given the presence of grease below. To achieve this, semi-flexible guide tubes can be used. This requires the insertion of the tube first. The probe is guided along the tube subsequently. Once the tip of the probe exits the guide tube, the inspection process starts. While this slows down the inspection and limits the viewable area, it allows for an inspection upwards.

Sampling of the grease at the lower anchorage zones can be conducted during the borescope inspection. For this, a semi-rigid aluminum wire can be inserted from the drain hole and advanced downwards until the grease is reached. The collected samples can be inspected for color, viscosity, and consistency.

The borescope inspection and grease sampling were completed on April 9, 2024. A dual camera VJ-4 video borescope, with a 6-mm diameter probe and 5-ft cable length, was used. The guide tube provided was too large to fit the drain hole. A semi-rigid aluminum wire was used instead after running it along the probe cable connected with electrical tape at approximately every foot. A segment of this wire was also used for the collection of grease samples. The items used in the inspection are presented in Figure 7.

Figure 7 Borescope setup used for the inspection.

In total, 14 stays were inspected (including Stays 1A, 3A, 5A, 7A, 10A, 13A, 16A, 18A, 20A, 1B, 4B, 7B, 11B, 13B) and more than 250 photos were taken. The complete photo deck may be downloaded from this link. A number of representative photos are presented in Figure 8.

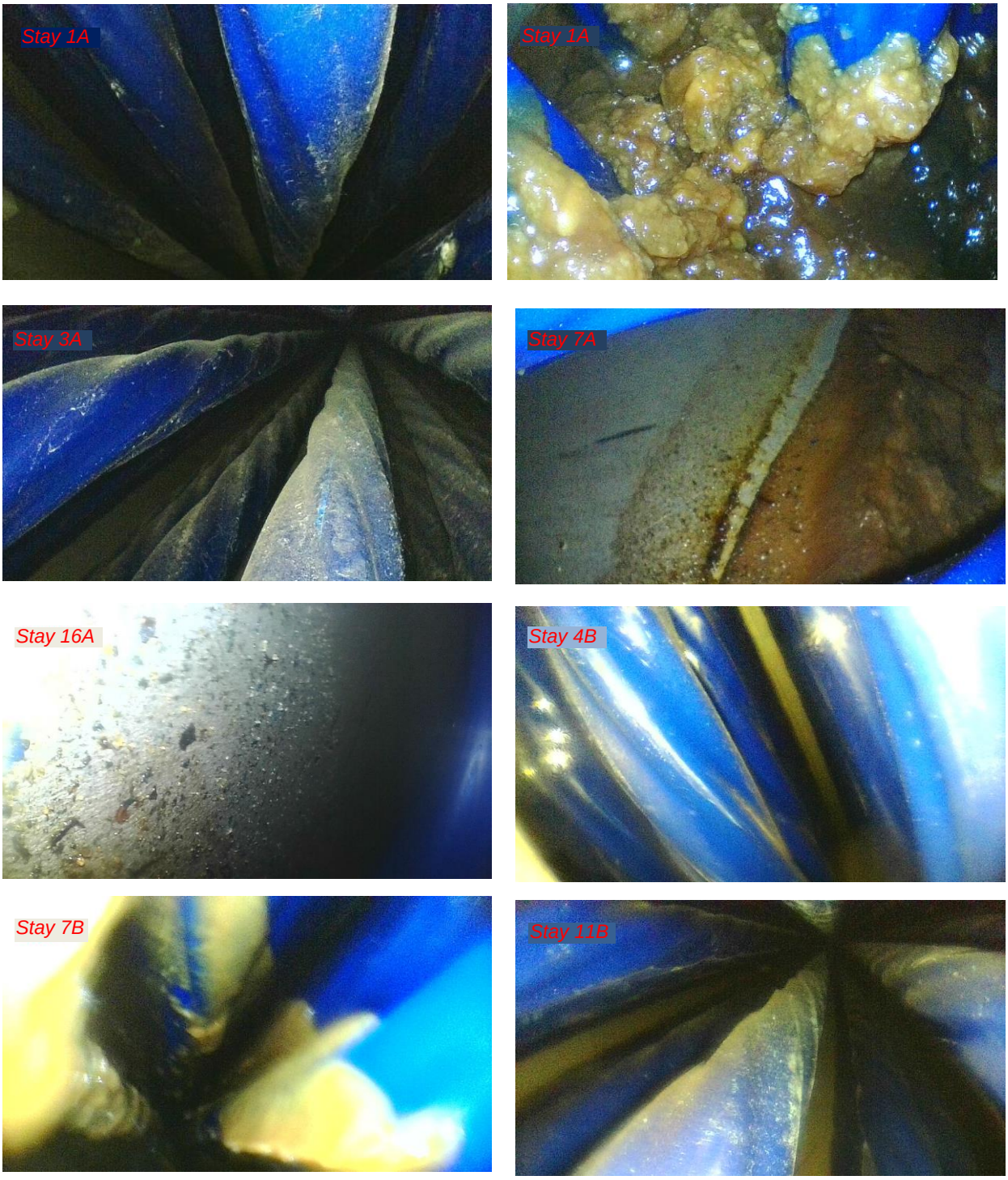

Figure 8 Representative photos from the borescope inspection.

In addition, grease samples were collected from ten stays and are presented in Figure 9.

Figure 9 Grease samples collected from the lower anchorage zones.

The inspected strands appeared to be in very good condition with no signs of epoxy coating damage, chipping, or corrosion. The dusty state of the strands implies no water runoff and dry conditions. The grease at the lower end of the stays appeared in good condition with no sign or presence of water. The collected grease samples appeared in very good condition with consistent color, viscosity, and consistency.

During the inspections, it was noted that not every B stay has a drain hole, while all A stays have drain holes. The stays without drain holes are 9B, 10B, 14B, 16B, 17B, 18B, 19B, 20B. It is recommended to add drain holes to these stays, matching the diameter and location of the existing ones.

4.2. Environmental Condition Monitoring Methods

As discussed in Section 3, moisture and oxygen are required for the corrosion process while the temperature affects the rate of corrosion. Monitoring the humidity and temperature conditions inside the stays can help assess the corrosion susceptibility of the internal environment. Various sizes of sensors and data loggers are available for continuously measuring and recording the humidity and temperature in a given environment. The research team conducted a review of these devices and communicated with two major suppliers, ONSET and Omega, to find the most suitable loggers for the VGCS. The probe-based sensors are found to be most suited. The probes can be selected small enough to fit the existing drain holes, while the data logger units can be selected to withstand the extreme environmental conditions that may be present during winter months. It is also important to use an external humidity and temperature data logger inside a radiation shield to monitor the ambient conditions.

The difference between the ambient and internal measurements is needed when assessing the conditions inside the stays (Figure 10 [8]).

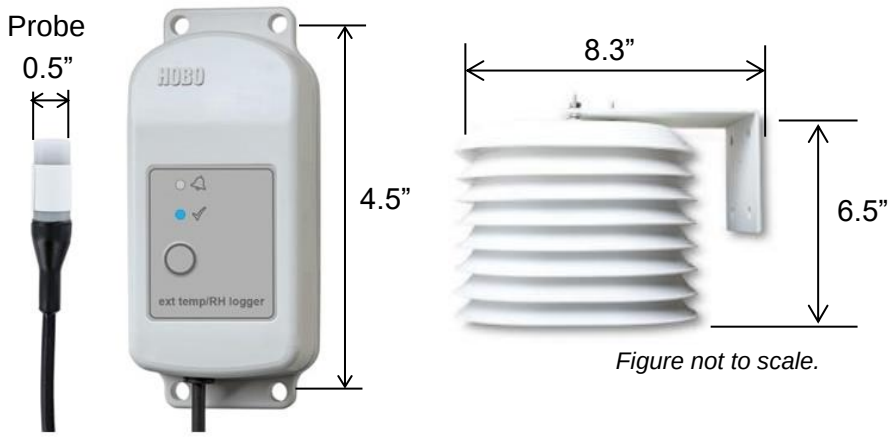

(a) Logger unit *(b) Solar radiation shield*

Figure 10 HOBO MX2300 series humidity and temperature logger used in this study.

The research team found Bluetooth connectivity to be the most suited among various connectivity options. This enables downloading the data wirelessly on site. In addition, these systems are more suited to extreme environments due to the lack of any USB or other cable connection ports for data downloading. The battery life of these devices ranges from one to five years, and the batteries are user replaceable. The higher end of the battery life is achieved by keeping the logger unit in a sleep state without transmitting the Bluetooth signal.

The instrumentation plan is presented in Figure 11. Two internal loggers and one external logger were included for contingency reasons. In total, six internal and two external loggers were installed. The internal sensors (HOBO MX2301A) have 6-ft probe cables with the temperature and humidity sensors attached at the tip. The external loggers (HOBO MX2302A) have an internal sensor without any probe cable. The battery life is specified by the manufacturer as five years with a logging interval of one minute and power saving mode enabled. The power-saving mode prevents loggers from broadcasting the Bluetooth signal continuously. This requires pressing the button on the logger, which will start the signal before downloading data using Bluetooth. The actual battery life was much shorter in this study, as will be discussed below. The memory allows a maximum of 84,650 measurements. This indicates that the memory will become full and require downloading in 59 days when 1-minute logging interval is used.

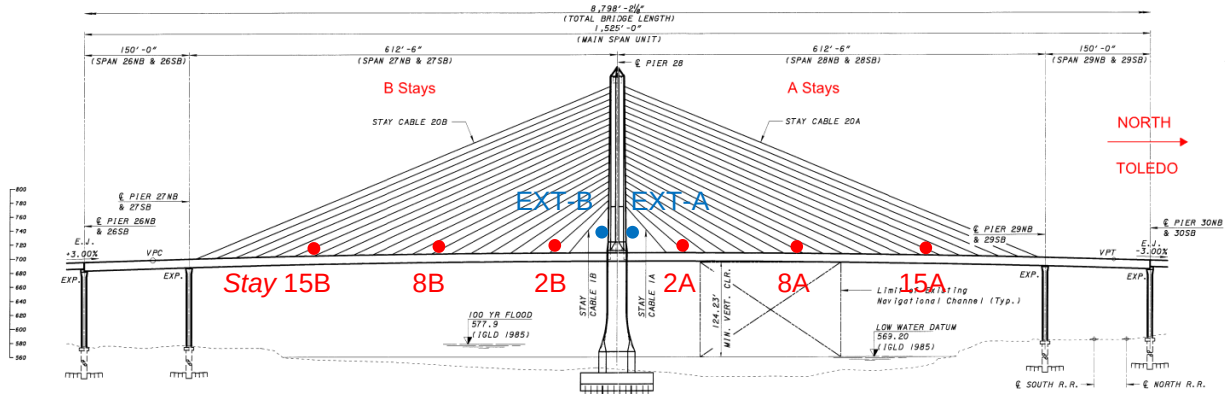

Figure 11 Instrumentation plan for the data loggers.

The existing drain holes were used for the insertion of the probes of the internal loggers. It was important to insert the probes upwards to prevent rainwater running along the cables and sensors from falling into the grease beneath. This was not possible with the thin and flexible probe cables. To increase their rigidity, 12-gauge aluminum wires were attached along the probe cables using electrical type, as was done in the borescope inspection. In addition, the combined probe cable and aluminum wire were placed in plastic wire loom auto-split tubing. This was necessary for preventing potential damage to the probe cable due to constant wind and traffic vibrations, especially at the drain hole where the cable goes inside the stay. High-quality straps were used to support the loggers and cable bundles outside the stays. Ample amounts of zip ties were used in the installation. The hardware used in the installation is presented in Figure 12. A sample installation and installed logger are shown in Figure 13.

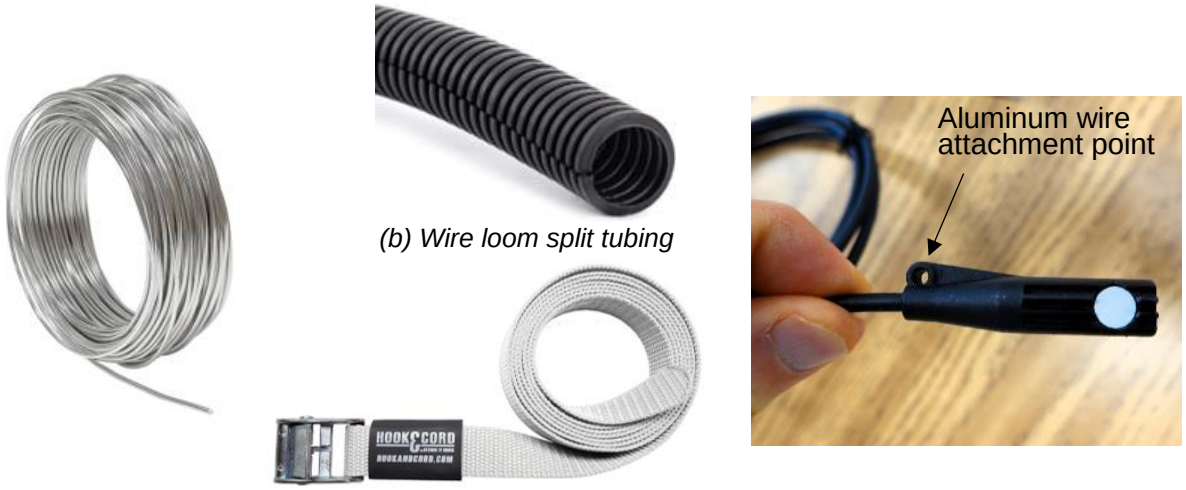

(a) 12-gauge aluminum wire *(b) Wire loom split tubing* *(c) Tie down lashing strap* *(d) Temperature and humidity sensor*

Figure 12 Hardware used for the logger installation.

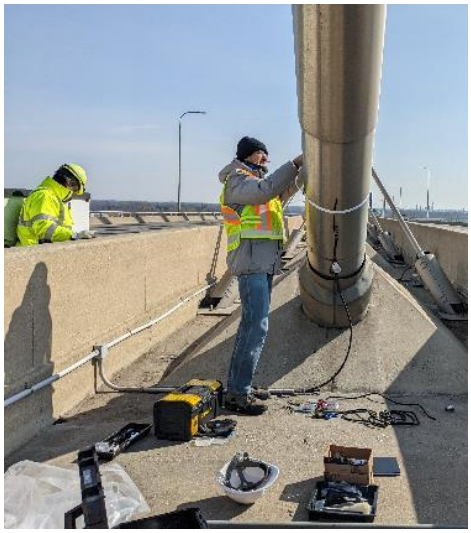

(a) Stay 2B

(b) Stay 15A

Figure 13 Internal logger installation on site.

The external loggers were installed inside the solar radiation shields manufactured for the specific logger model used. The purpose of this shield is to block direct sun exposure and create a consistent measurement environment for both external loggers. One external logger/radiation shield bundle was installed at each side of the pylon using concrete screws (Figure 14).

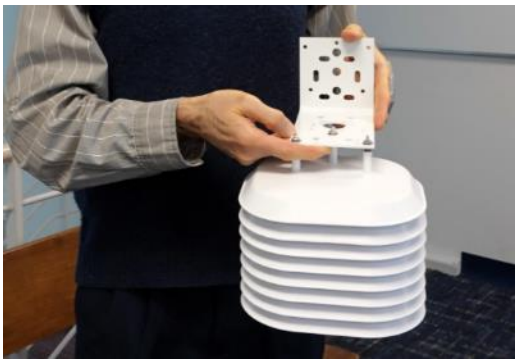

(a) External logger-radiation shield bundle

(b) Installation on the pylon (EXT-B)

(c) External logger-radiation shield bundle installation locations (B side is shown)

Figure 14 External logger installation on site.

All loggers were initialized with 30-minute logging intervals. This interval records 48 measurements per day and is sufficient for the project's purpose. Another benefit is the increased battery life and 1,763 days (or 4.8 years) of recording before the memory becomes full. Consequently, the data download can be made at any desired intervals (planned as 6 months) without running the risk of a memory-full situation.

It was planned to collect data for one year to assess the seasonal changes in internal humidity and temperature. Based on the results, the sensors could be removed, left installed for more data collection, or moved to other high-risk locations such as the saddle ends of the stays at the pylon.

The loggers were installed on February 28, 2024. The first data download took place on April 9. All loggers were working as intended on this date. During the subsequent data download on November 7, 2024 (Figure 15), it was noted that the logging interval was reset to one minute after the data download on April 9. This caused the memory to be full on May 1, and no further recording could be made after this date. This arbitrary change in the configuration after data download may be noted as one weakness, or a bug, of the software controlling the loggers. The software did not give any warning or notification for this configuration change.

During the data download on November 7, Logger 15B was found non-operational due to battery drain. The logger was removed and taken back to the lab. The data was still available (until May 1) once the battery was replaced. This raised a concern about imminent battery drain with the remaining loggers; therefore, a battery-replacement site visit was scheduled for November. 26. It should be noted that the manufacturer’s specified battery life expectancy is five years, whereas the batteries lasted about nine months. The date of manufacture is stated as November 2022 on the batteries. This indicates a two-year battery life, including the time that non-recording loggers were waiting on the shelf.

A subsequent site visit was made on November 26 to replace the batteries of all loggers. Six internal logger batteries were replaced. Replacing the two external logger batteries requires the use of a ladder and disassembling the radiation shields. This was not done due to cold and windy conditions. The data from November 7 to 26 was also downloaded during this visit. The data showed that the humidity sensor of Logger 8B had malfunctioned, with no humidity data recorded. The batteries of the external sensors were replaced on January 30, 2025. During this visit, the data from all loggers were also downloaded. The data showed that Logger 8B had stopped working on January 18, 2025, with no temperature or humidity data recorded afterwards.

A final site visit was made on April 11 to download the logger data. The data showed that Logger 2B had malfunctioned with the data recorded until March 31. This experience confirms the need to include a few extra loggers for contingency reasons, as was done in this study.

The obtained data duration is 31.5 weeks (approx. 7.5 months) from February 26 to May 1, 2024, and November 7, 2024, to April 11, 2025.

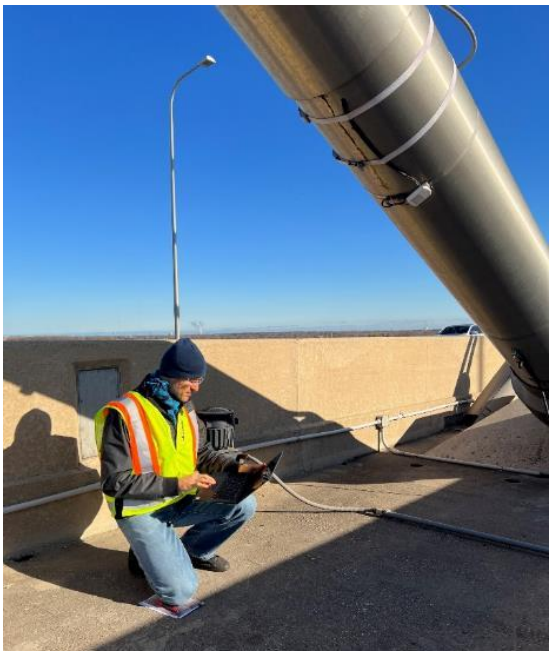

(a) Data downloading on Nov 7, 2024.

(b) Battery replacement requires the opening the back cover held by four screws.

Figure 15 Logger data downloading and battery replacement.

The recorded temperature data is presented in Figure 16. The temperature inside the stays is typically higher than the external temperature, with a maximum difference of 23˚F for the A stays and 19˚F for the B stays.

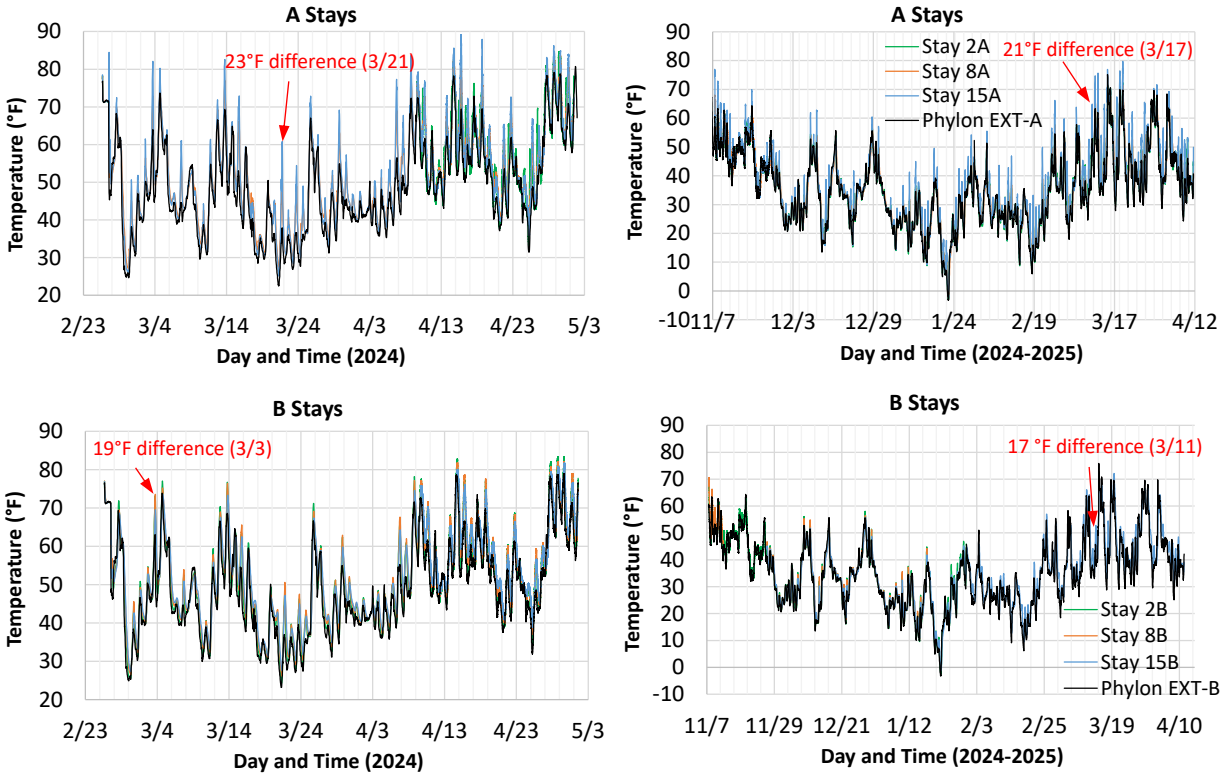

Figure 16 Temperature data collected.

The recorded relative humidity (RH) data is presented in Figure 17. The RH inside the stays is typically less than the RH outside. The use of RH is misleading when assessing moisture under different internal and external temperatures. RH is a relative measure of moisture as compared to how much moisture that air can hold at that temperature.

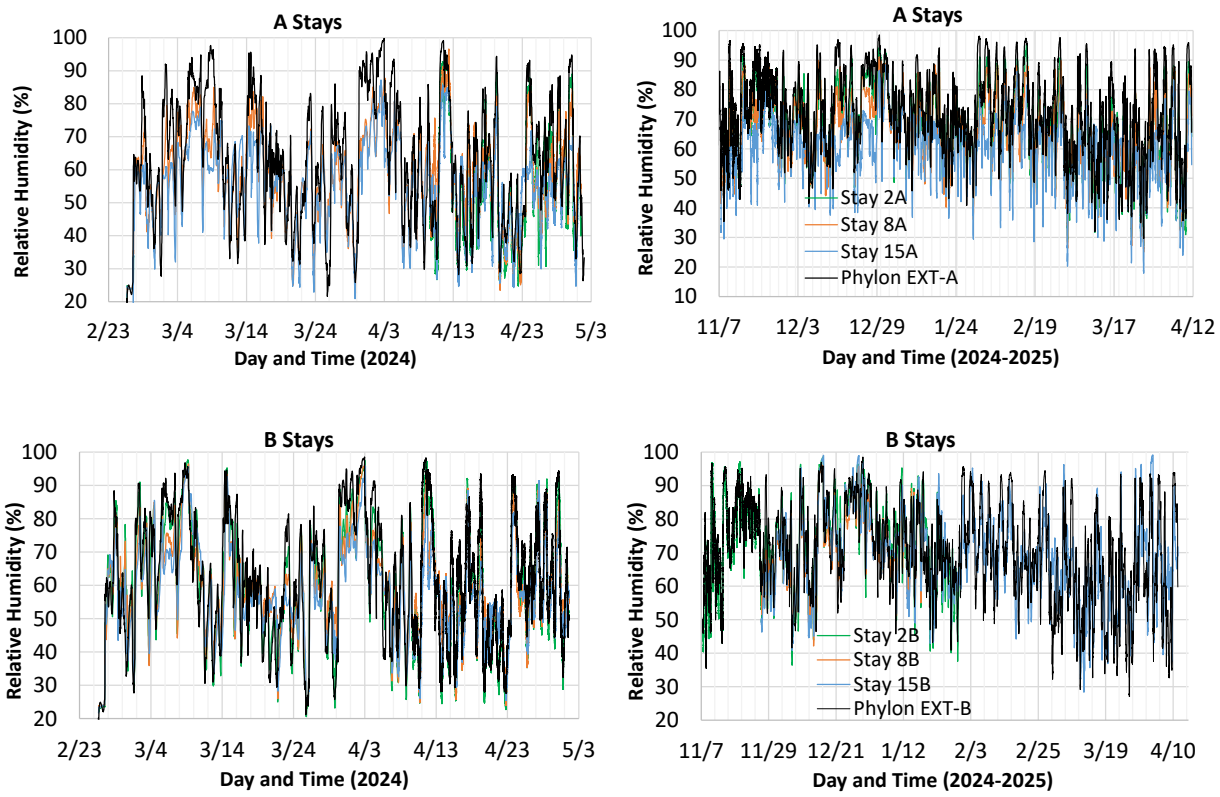

Figure 17 Relative humidity data collected.

As shown in Figure 18 [9], higher temperatures hold larger amounts of moisture. It is important to consider the temperature when assessing the amount of moisture inside the stays as compared to outside. Dew point, which is an absolute measure of how much moisture is in the air, is a better suited quantity for this purpose.

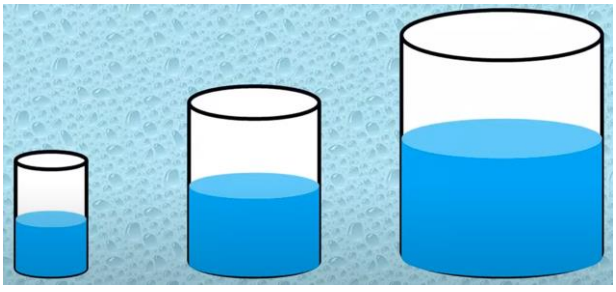

Temp =	55°F	75°F	95°F
RH=	50%	50%	50%
DP=	37°F	55°F	74°F

Dew Point (°F)	How it Feels
>75	Oppressive
70-75	Very humid
65-69	Humid
60-64	Slightly humid
55-60	Comfortable
<55	Dry

Figure 18 Dew point versus relative humidity.

The calculated dew point (DP) data is presented in Figure 19. This calculation uses the temperature and relative humidity as input. The DP inside the stays is generally higher than the external DP, with a maximum exceedance of 20°F for the A stays and 24°F for the B stays. This indicates that the B stays have more moisture than the A stays. The maximum exceedance is generally at lower DPs, as shown in Figure 20. The overall condition of the stays may be categorized as slightly humid, according to the table in Figure 18 [10].

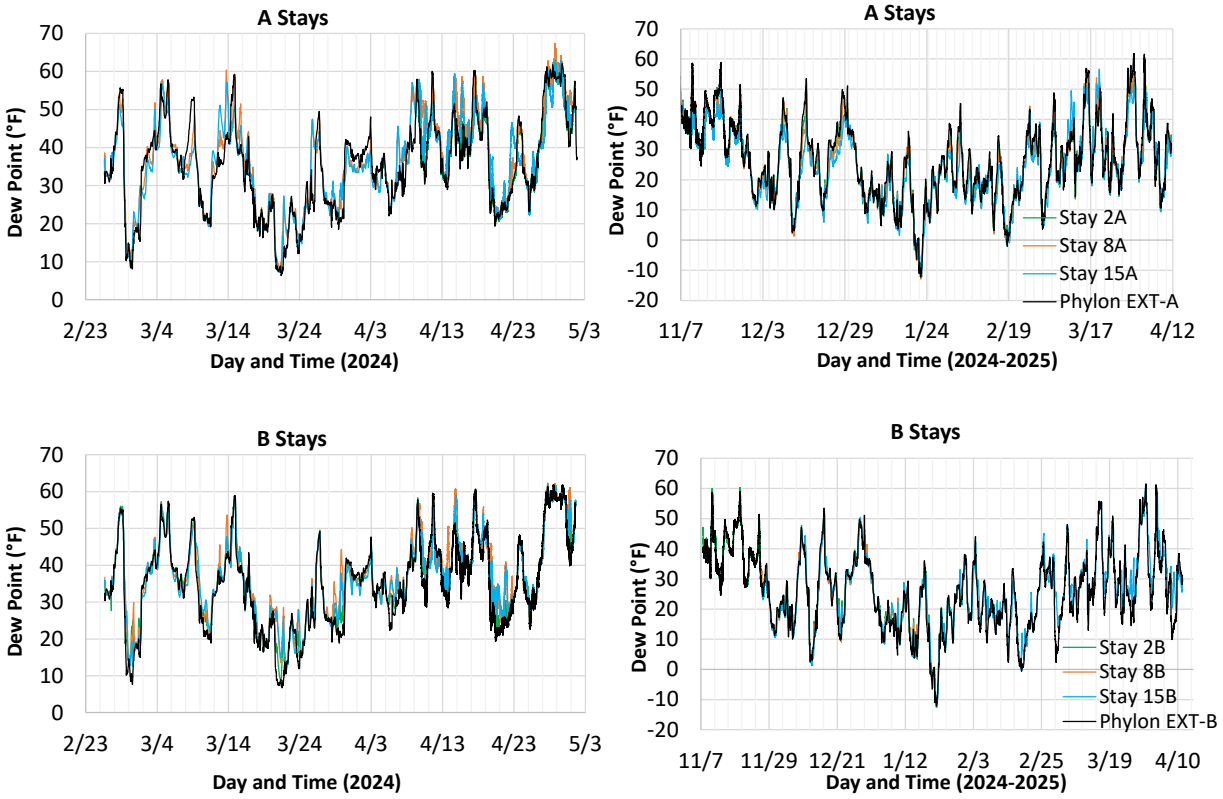

Figure 19 Dew point variation (calculated from the data collected).

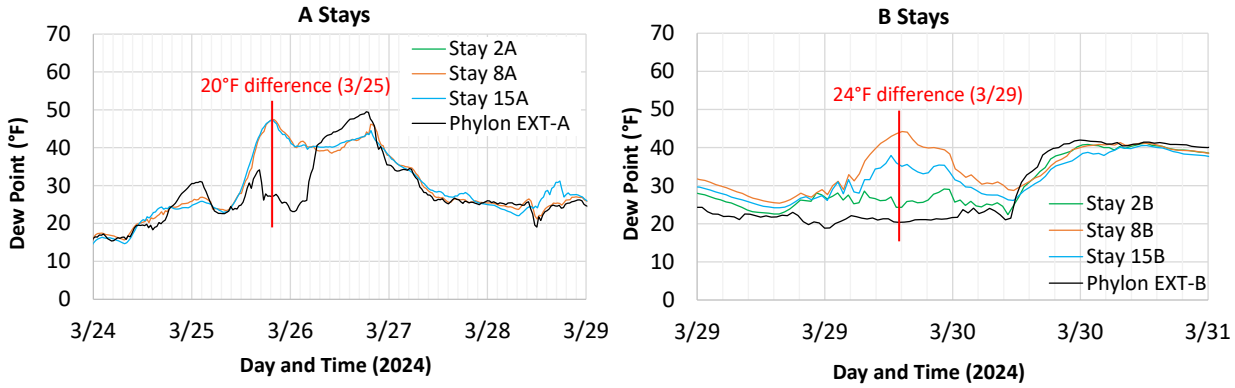

Figure 20 Dew point maximum exceedance inside stays compared to outside.

To assess the measurement consistency, both of the external logger's data is plotted in Figure 21. The coincidental lines confirm the consistency.

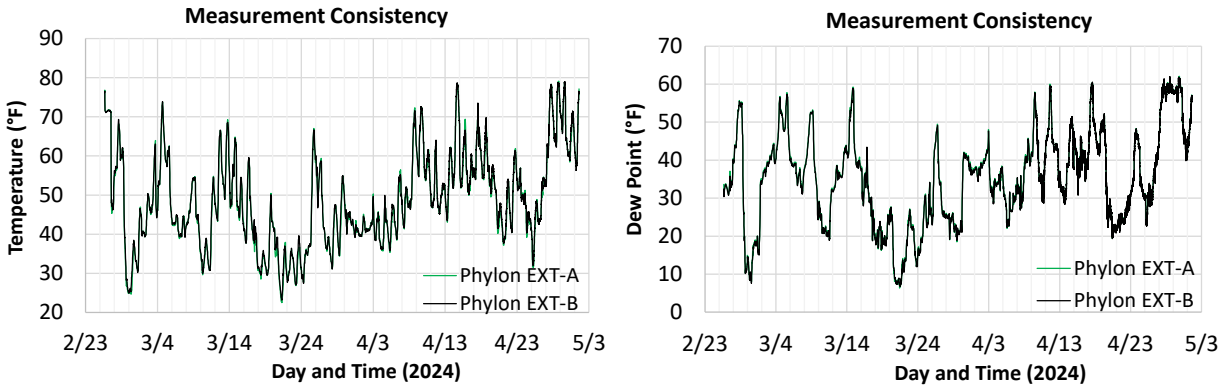

Figure 21 Measurement consistency between two external loggers.

The external logger A was operational with a 30-minute logging interval from May 1 to November 7, 2024, when no other logger was operational. Figure 22 shows that the more humid months are from the beginning of June to the end of September. The maximum external dew point recorded corresponds to very humid ambient conditions.

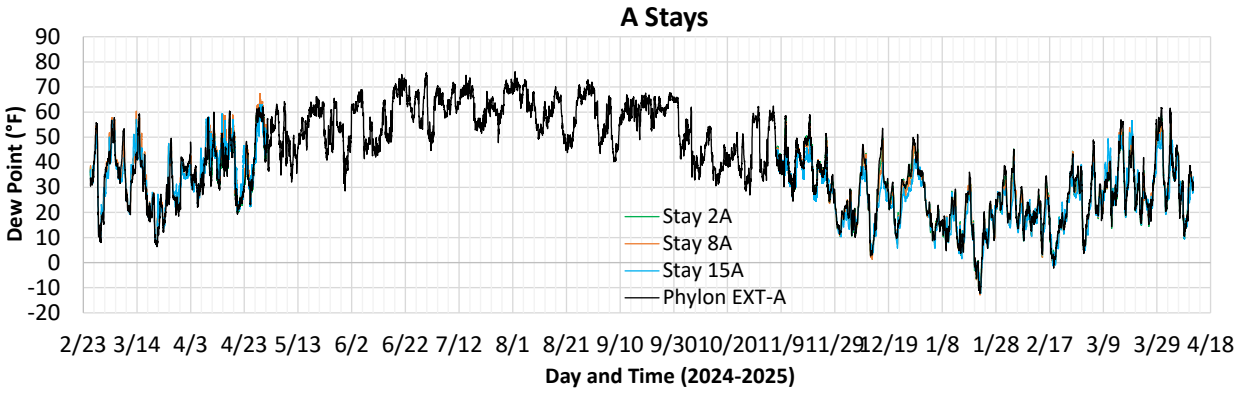

Figure 22 Full extent of data collected by the external logger A.

An overall assessment of the data indicates that the conditions inside the stays are slightly more humid than the ambient (outside) conditions. There is no evidence of excessive moisture accumulation inside the stays.

4.3. Vibration Methods

Variation of forces and other dynamic characteristics of cables can not only indicate their condition but also damage at any other location in a cable-stayed bridge [11]. Damage and changes at any location on the cable-stayed bridges induce changes in the force distribution of all members, including the cables. Therefore, consistency of cable tensions over time is considered one of the health indicators for both cables and the superstructure [12–14]. Cable tension can be measured directly [15] or estimated by measuring different parameters of the cable, such as stress [16], strain [17], or natural frequencies [18]. The methods that use cable natural frequencies to estimate the cable tension are called the vibration-based tension estimation methods [19–22]. The

vibration-based methods have been extensively employed to estimate the cable tensions and bridge health in many cable structures around the world [23–25] (Figure 23 [11]).

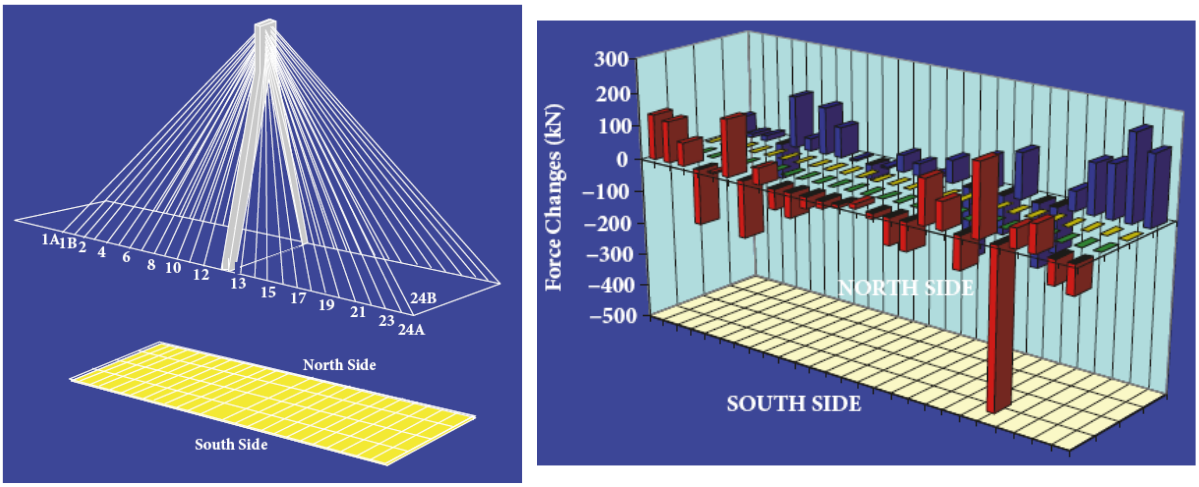

(a) Schematic of a cable-stayed bridge *(b) Force variation in cables from the baseline values*

Figure 23 Health monitoring of stay cables using vibrational methods.

The simplest model of a vibrating stay assumes that it behaves like a taut string, neglecting both sag extensibility and bending stiffness. The following equation relates the taut string frequencies and tension:

$$f_n = \frac{n}{2L}\sqrt{\frac{T}{m}} \qquad (1)$$

f_n n^{th} harmonic frequency (Hz)
n harmonic number
T tension in the string (N)
L cable length (m)
m cable mass per unit length (kg/m)

To determine the tension force in a vibrating stay using Eq. (1), one needs to measure its harmonic vibration frequencies. The other parameters are constants and can be determined from the design drawings.

Vibration frequencies are commonly measured using accelerometers attached to stays at their lower accessible ends. This method requires the temporary installation of one to two accelerometers on a stay and recording of data for a few minutes (Figure 24 [18]). In most cases, the ambient excitation sources, such as traffic and wind induce enough vibrations, and there is no need for manual excitation. This method was applied to the VGCS after its construction and a few concerns were raised, including the interference of the dampers, and the sheathing vibrating somewhat differently than the strands at the lower ends of the stays [26].

Figure 24 Accelerometer testing performed on VGCS stays after construction.

Another method to determine the vibration frequencies is to use a laser vibrometer (e.g., [11]). This method is commonly used in mechanical engineering, but its use in bridge engineering remains limited. A possible reason for this may be the high cost of a laser vibrometer and the unfamiliarity of civil engineers with theory of vibration.

In traditional grout-filled stays, the sheathing and strands vibrate as a unit. This allows taking frequency measurements, either using accelerometers or a laser vibrometer, from the accessible lower ends of the stays. The previous studies on the VGCS found that the non-grouted strands and sheathing may not vibrate as a unity at the lower ends of the stays, and the damper connections at these locations may interfere with the measurements [18,27]. Therefore, measurements taken on the sheathing from these locations may not represent the vibrational behavior of the strands. This makes it necessary to obtain measurements from the middle (or central one-third) lengths of the stays (Figure 25). Running electrical cables and installing accelerometers at these locations present a major challenge; therefore, the laser vibrometer method is much more practical for the VGCS.

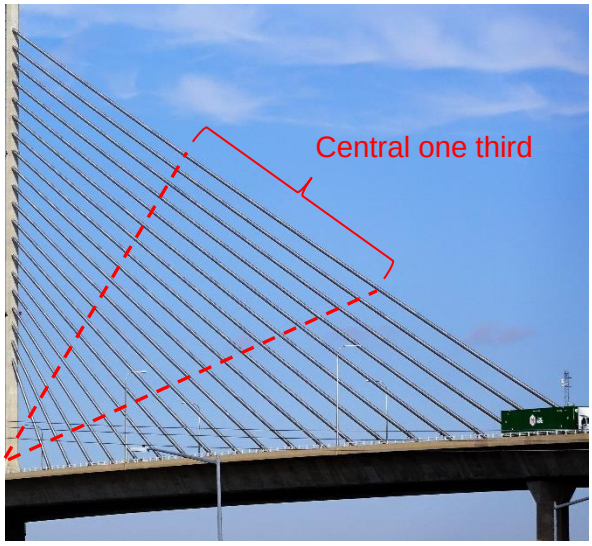

Figure 25 Recommended vibration measurement locations for the VGCS.

The laser vibrometer test setup used in this study is presented in Figure 26. It consists of a vibrometer, a lens, a precision tripod, a power source, and a laptop for data acquisition. The lens used in this study had a maximum range of 100 m (328 ft); other lenses were on special order (Figure 27).

Figure 26 Laser Vibrometer test setup used.

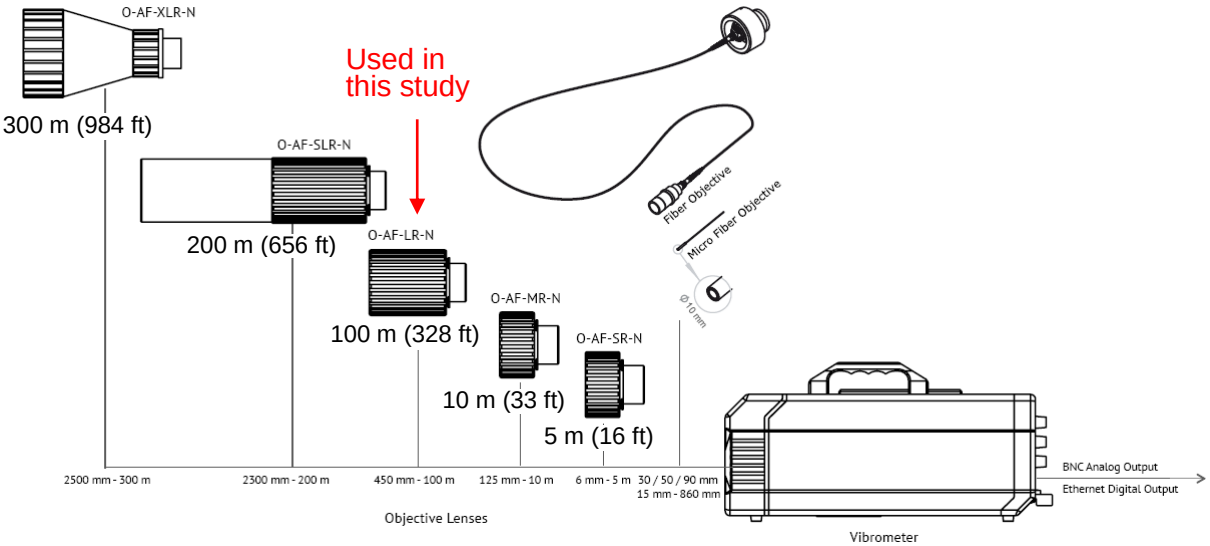

Figure 27 Ranges of the lenses compatible with the vibrometer used.

To test the experimental setup, a pilot measurement study was undertaken from the Robert Craig Memorial Bridge on July 27, 2024, benefiting from the closed state of this bridge due to an earlier accident. The vibrometer setup locations are shown in Figure 28. The research team realized that it was not possible to see the laser beam even at

a short distance on the pavement due to bright sunlight (Figure 29) and decided to come back before dusk to test the visibility before and after the bridge illumination.

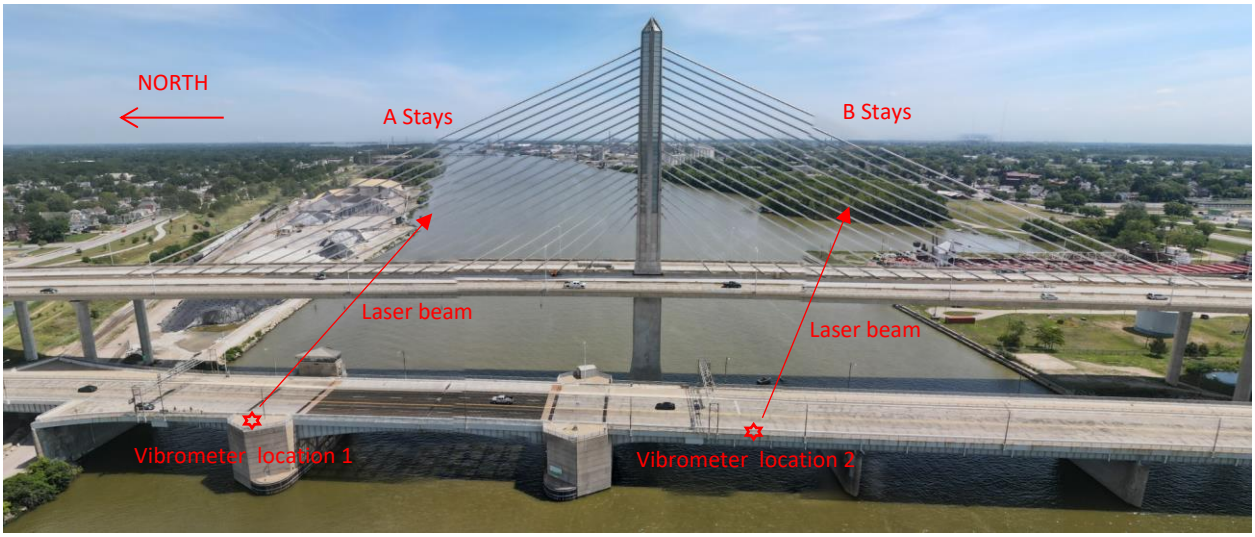

Figure 28 Pilot study setup locations on the Robert Craig Memorial Bridge.

Figure 29 Invisible laser beam on the pavement.

It was possible to see the laser beam both before and after the bridge illumination with the help of a pair of binoculars (Figure 30). Due to the unavailability of the scope accessory, the team temporarily installed general-purpose binoculars on the vibrometer, offset by a firm foam. The scope accessory is recommended for any subsequent measurements. The signal strength, which is a measure of the reflected laser beam that is received back by the vibrometer, was poor in all measurements (Figure 30). Possible reasons for this may be the distance that exceeded the lens range (not measured), the aiming angle that reduced the reflected signal, or a combination of both. Since the objective was to test the setup before the actual measurements from the deck of the VGCS, the measurement accuracy was not a major concern. To the surprise of the research team, however, the measured frequencies correspond very well with the baseline values, as will be discussed at the end of this section.

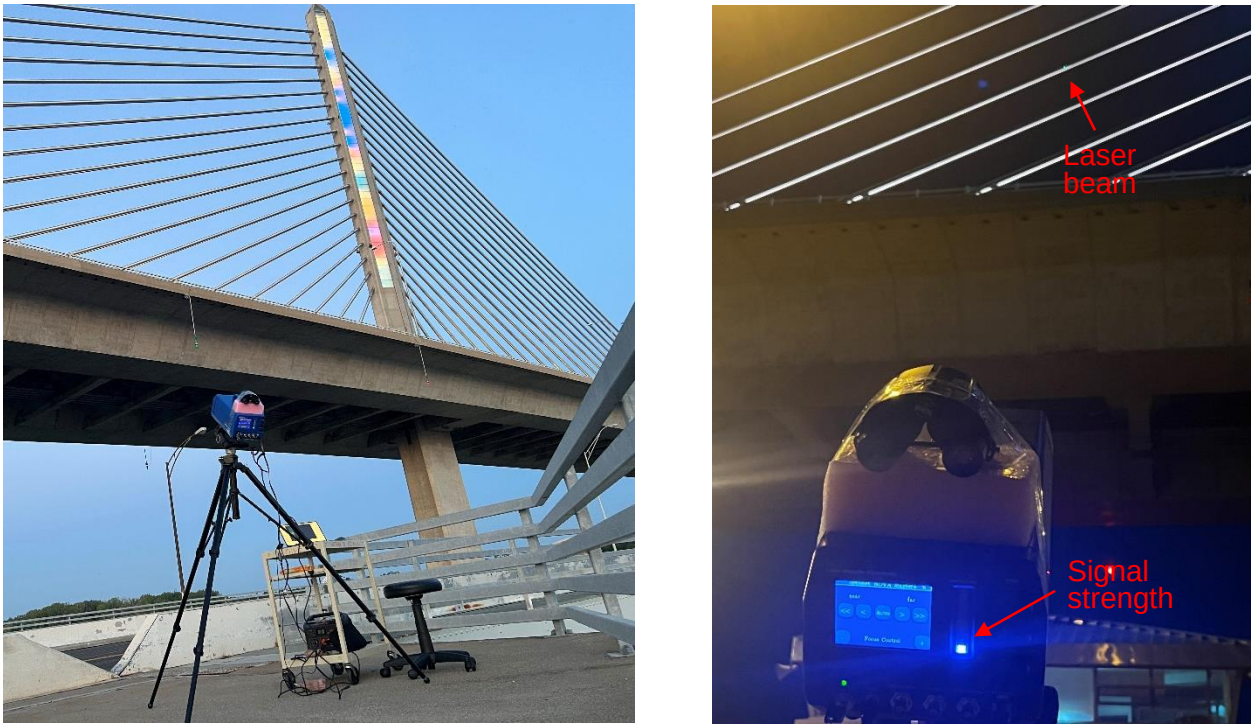

Figure 30 Measurements from the Robert Craig Memorial Bridge before and after dusk.

The actual measurements were taken from the deck of the VGCS on July 30, 2024. ODOT arranged the closure of the right lane to provide a suitable workspace and reduce the high-pressure shockwaves and deck vibrations associated with passing trucks. The traffic was light, and the weather was well suited to conduct site work, with 5 mph wind, and 74˚F (23˚C) temperature, which decreased a few degrees as the night advanced. The test setup is shown in Figure 31.

Figure 31 Test setup on the deck of VGCS at the north of the pylon.

The sampling included even numbered stays, which resulted in a 50% sampling rate. Ten stays on the north of the pylon (named A stays), and 10 stays on the south of the pylon (named B stays) were measured. In all measurements, sufficient signal strengths were obtained. Multiple measurements were taken at each stay to obtain high-quality data, which reduces the effects of the passing trucks and contains less noise. It was found that a minimum recording duration of 30 seconds is required for each measurement. The longer recording durations are useful in reducing the effects of passing trucks and associated noise since these events occupy a smaller proportion of the entire recording as the recording duration is increased. Consequently, a recording duration of 45 or preferably 60 seconds is recommended for any future measurements.

The measurements were taken at the central one-third length of each stay. It was confirmed, through multiple measurements for each stay, that changes in the measurement location did not influence the measured vibrational frequencies. As a sample, the measurement location and associated recording for Stay 16B are shown in Figure 32 and Figure 33.

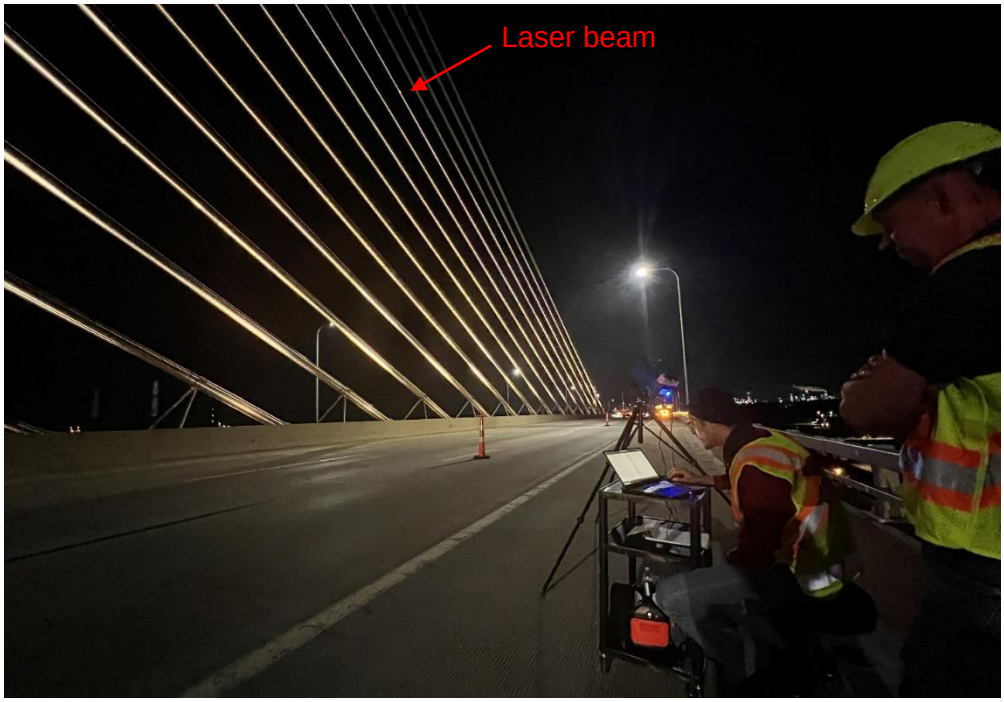

Figure 32 Stay 16B is aimed at its central one-third length.

The presence of deck vibration is a source of concern for laser vibrometer measurements taken from the deck. As the deck vibrates, the vibrometer also vibrates. If the deck's natural vibration frequency happens to be similar to a stay's frequency, a phenomenon called 'resonance' occurs. This invalidates the recording. To investigate this issue, the deck vibration is measured, and the first natural frequency was found to be approximately 7.5 Hz (see Figure 34). This value corresponds well with the value obtained from the Robert Craig Memorial Bridge (7.0 Hz) a few days earlier. Since the measured stay frequencies range from 0.6 to 3 Hz, resonance or any major influence of the deck vibrations is not expected.

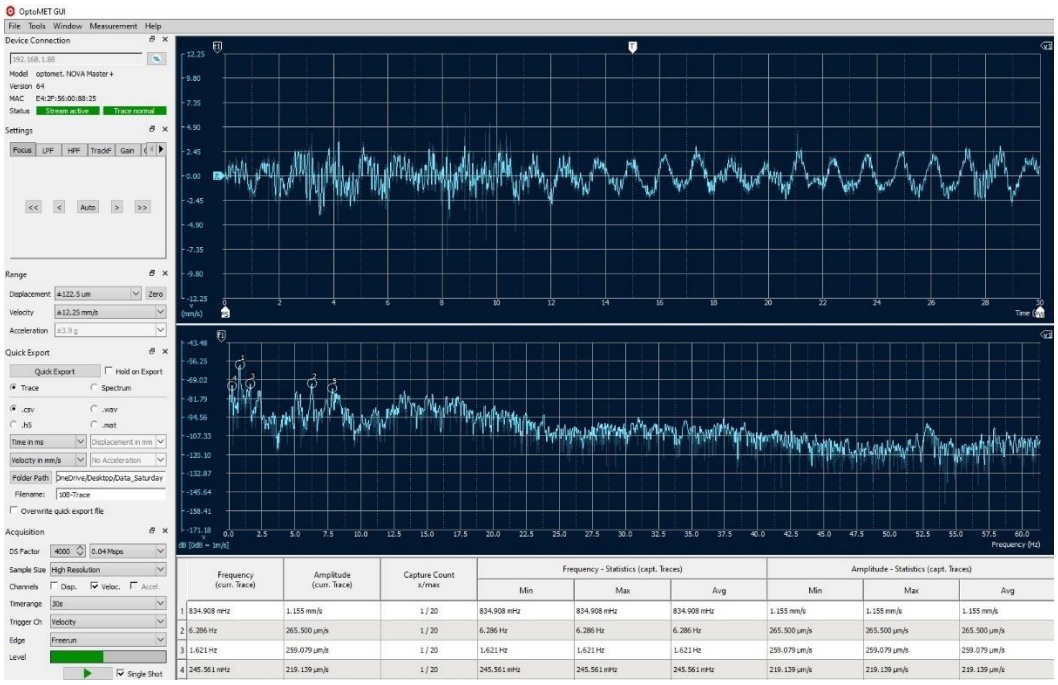

Figure 33 Velocity histogram and frequency spectrum obtained for Stay 16B (f_1 = 0.835 s).

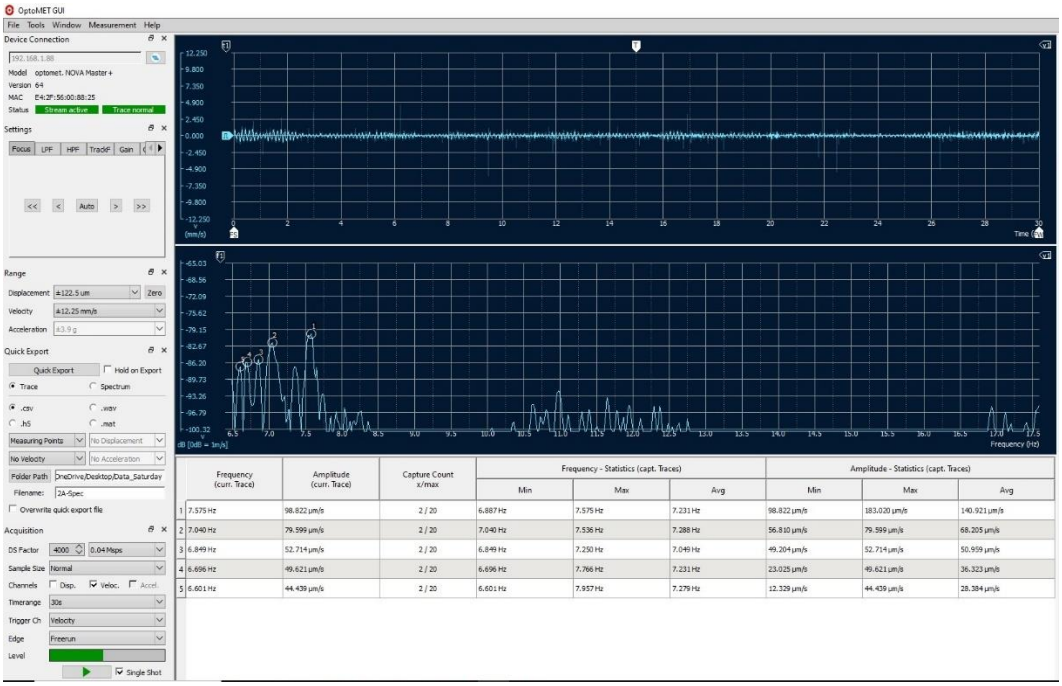

Figure 34 Velocity histogram and frequency spectrum obtained for the deck (f_1 = 7.575 s).

The force in each stay was calculated using Eq. (1), where n is taken as 1 and f_1, the first natural vibration frequency, was measured with the vibrometer as described above. The constant stay properties (i.e., cable length and mass) and the sheath mass participation factors were obtained from the earlier studies conducted on this bridge [18,27]. The sheath mass participation factors account for the sheath and strand bundle interaction. The calculated stay forces are presented in Table 1.

Table 1 Calculated stay forces at an ambient temperature of 74°F.

Stay	L (m)	No of Strands	Steel Area (mm^2)	f_1 (Hz)	Force (kN)
2A	36.6	82	11484	3.039	5,543
4A	53.6	105	14710	2.254	9,164
6A	71.4	120	16774	1.743	10,694
8A	89.4	131	18323	1.422	12,763
10A	107.2	149	20839	1.158	13,610
12A	125.3	150	21032	1.029	14,266
14A	143.3	156	21871	0.904	14,846
16A	161.4	156	21871	0.856	17,170
18A	179.5	139	19484	0.718	13,770
20A	197.5	116	16258	0.649	10,983

Stay	L (m)	No of Strands	Steel Area (mm^2)	f_1 (Hz)	Force (kN)
2B	36.6	82	11484	2.910	5,425
4B	53.6	105	14710	2.281	8,948
6B	71.4	120	16774	1.791	11,543
8B	89.4	131	18323	1.420	12,443
10B	107.2	149	20839	1.164	13,570
12B	125.3	150	21032	1.011	13,976
14B	143.3	156	21871	0.904	14,832
16B	161.4	156	21871	0.835	15,885
18B	179.5	139	19484	0.725	13,757
20B	197.5	116	16258	0.651	10,805

As per Eq. (1), stay forces are proportional to the square of the measured frequency, given that other terms are constant. For any future measurements in the following years, the following equation may be used to calculate the stay forces without the need to substitute the constant term.

$$Force_{(future)} = \left(\frac{f_{1(future)}}{f_{1(this\ study)}} \right)^2 \times Force_{(this\ study)} \qquad (2)$$

The lift-off values, measured by the contractor in 2007 using a load cell, were obtained from the spreadsheets provided by ODOT. These values are considered to represent healthy baseline conditions and will be compared with the calculated tensions. It is necessary to apply a temperature adjustment before this comparison.

Temperature affects the force in a strand. Higher temperatures result in a reduction in strand tensions; therefore, the calculated tensions should be adjusted for the temperatures during the lift-off measurements. The contractor sheets specify the strand temperatures during the measurements. For some stays, two values are reported. As an example, the strand temperatures reported for Stay 15B are presented in Table 2. For such stays, the average value is used.

Table 2 Sample temperatures specified in contractor's lift-off sheets,

Stay 15 Temperatures			
Stay Strands (shade/sun)	49/64	Stay Sheathing (shade/sun)	50/60

The thermal force change relationship used for the adjustment of stay forces is given by the following equation.

$$\Delta F = E \cdot A \cdot \alpha \cdot \Delta T \qquad (3)$$

where ΔF is the change in the stay force (N) due to a temperature change of ΔT (°C), E is the modulus of elasticity of the strands (200,000 MPa), A is the total area of the

strands in a stay in mm^2, and a is the coefficient of thermal expansion of the strands (11.5×10^{-6} 1/°C).

The temperature-adjusted stay forces are compared with the lift-off forces in Table 3, where the deviation percentages from the baseline lift-off values are shown. A positive deviation indicates that the estimated force is larger than the baseline value, while a negative deviation indicates the opposite. Large deviations are obtained for Stays 2 and 4. These are the shorter and stiffer stays. The strands and sheathing do not vibrate as a unit; therefore, the frequency measurements obtained from the sheathing, where the laser signal is aimed, do not represent the frequency of the strand bundle. Consequently, for Stays 1 to 4, stay force estimations by measuring the sheathing vibrations may not be possible. A similar conclusion was also reached in the earlier studies conducted on this bridge [18,27]. In the subsequent measurement, it is recommended to aim the laser beam at a cheese plate location for these shorter stays, where the strand bundle and sheathing may vibrate as a unit, to assess the influence of this location on the measured frequency.

Table 3 Comparison of the calculated stay forces with lift-off forces at the same temperature.

Stay	T (°C)	Steel (mm^2)	Force (kN)	T (Lift-off, °C)	ΔF (kN)	Force+ΔF(kN)	Lift-off (kN)	Deviation
2A	23	11484	5,543	2	549	6092	8,097	-25%
4A	23	14710	9,164	1	741	9905	8,094	22%
6A	23	16774	10,694	1	844	11539	10,864	6%
8A	23	18323	12,763	17	243	13006	12,602	3%
10A	23	20839	13,610	14	423	14033	12,744	10%
12A	23	21032	14,266	9	683	14949	13,805	8%
14A	23	21871	14,846	6	878	15723	15,813	-1%
16A	23	21871	17,170	11	598	17768	17,386	2%
18A	23	19484	13,770	3	894	14664	14,998	-2%
20A	23	16258	10,983	-4	1005	11988	11,794	2%

Stay	T (°C)	Steel (mm^2)	Force (kN)	T (Lift-off, °C)	ΔF (kN)	Force+ΔF(kN)	Lift-off (kN)	Deviation
2B	23	11484	5425	9	373	5,798	7913.9	-27%
4B	23	14710	8948	9	477	9,426	10342.5	-9%
6B	23	16774	11543	8	587	12,131	11802	3%
8B	23	18323	12443	10	548	12,991	12987.1	0%
10B	23	20839	13570	6	836	14,406	14094.4	2%
12B	23	21032	13976	9	683	14,659	14254	3%
14B	23	21871	14832	13	500	15,333	14921.4	3%
16B	23	21871	15885	11	584	16,469	17242.9	-4%
18B	23	19484	13757	5	807	14,564	14131.3	3%
20B	23	16258	10805	1	819	11,623	12748.4	-9%

For the remaining 16 stays, the deviation of temperature-adjusted stay forces from the lift-off forces are presented in Figure 35. All deviation values are under 10%, which is within the margins of expected deviation. There are inherent errors built into the calculation and measurement procedures. The taut string equation, for example, neglects the bending stiffness of the stays. The temperature effects are considered approximate given the variable temperatures of the stays depending on their location (e.g., north or south) and sun or shade conditions. The laser vibrometer measurement method may introduce ±1% error, which corresponds to ±2% error in the estimated stay forces (Mehrabi and Farhangdoust 2018). The lift-off values may also have minor errors involved. Consequently, the results do not warrant a credible concern for the health of the strands.

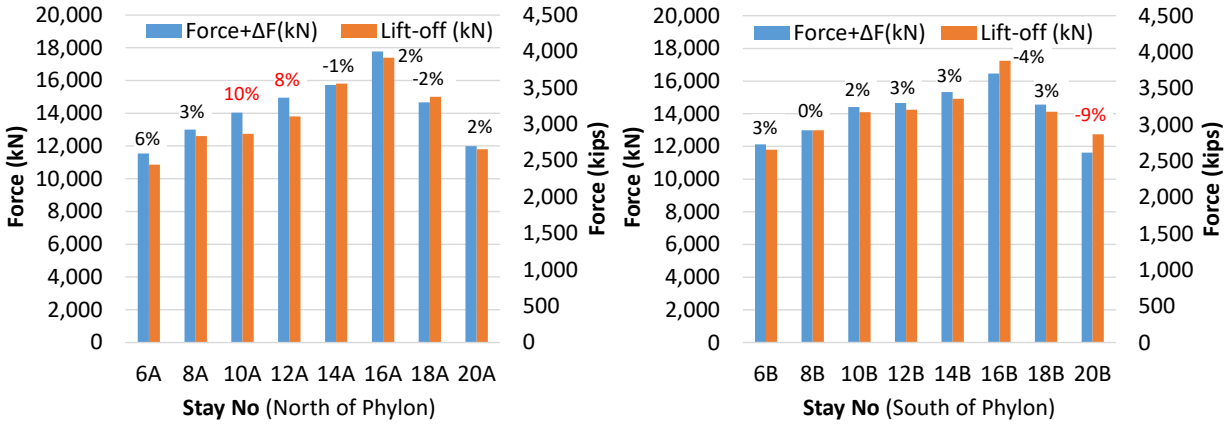

Figure 35 Comparison of the calculated stay forces with lift-off forces at the same temperature.

The frequencies measured from the Robert Craig Memorial Bridge are also used to calculate the stay forces. The calculated forces correspond well with the lift-off values despite the poor signal strength. Figure 36 shows the comparison of temperature-adjusted stay forces with the lift-off forces, including the measurements taken from the Robert Craig Memorial Bridge.

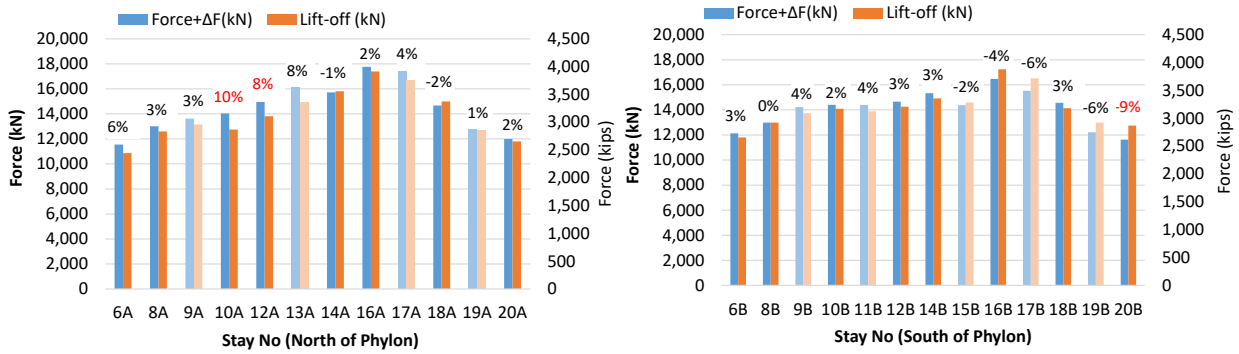

Figure 36 Comparison of the calculated stay forces with lift-off forces at the same temperature, including measurements from the Robert Craig Memorial Bridge (shown with faint colors).

While within the margins of expected deviation, the 10% and 8% overestimation of Stays 10A and 12A indicate a need to monitor this area in the next measurement cycle. If, at that time, the force in Stay 11A (not measured in this study) is found notable below its

lift-off value, this may indicate a concern. A common pattern for potential damage includes a stay losing its tension and two adjacent stays gaining tension. The 9% deviation measured for Stay 20B is less of a concern, given that the Stay 19 measurement from Robert Craig Memorial Bridge also has a deviation in the same direction.

Considering the results obtained and the error margins built into the procedures, no credible concern is detected for the health of the stay cables of the VGCS. It is recommended that a re-measurement study is undertaken in 4 years with closer attention to Stays 10A-11A-12A and 18B-19B-20B. Laser vibrometer measurements from the Robert Craig Memorial Bridge may be considered at that time if an extra-long-range lens and proper aiming equipment could be secured. This may eliminate the need to close a lane of the VGCS. In addition, measurements could be split into two nights for a longer duration and multiple rounds of recordings.

4.4. Magnetic Methods

Magnetic Flux Leakage (MFL) is identified as an applicable method for the free lengths of the stays [28]. MFL uses a magnet to directly magnetize the ferrous material (steel) within the sheath (Figure 37 [29]). This induces flux paths in the material between the two poles of the magnet. Where section loss is present, the magnetic field in the material 'leaks' from its typical path of least resistance. A magnetic field detector (comprised of Hall effect sensors) between the poles of the magnet is sensitive to this change in magnetic field and indicates the leak. MFL can locate strand defects in both metal and nonmetal external ducts with moderate to high accuracy; however, it cannot differentiate between corrosion, section loss, and breakage. It can locate corrosion, section loss, and breakage with a loss in metallic area greater than 5 to 10% [2]. This notable amount indicates that MFL may not detect superficial or surface corrosion.

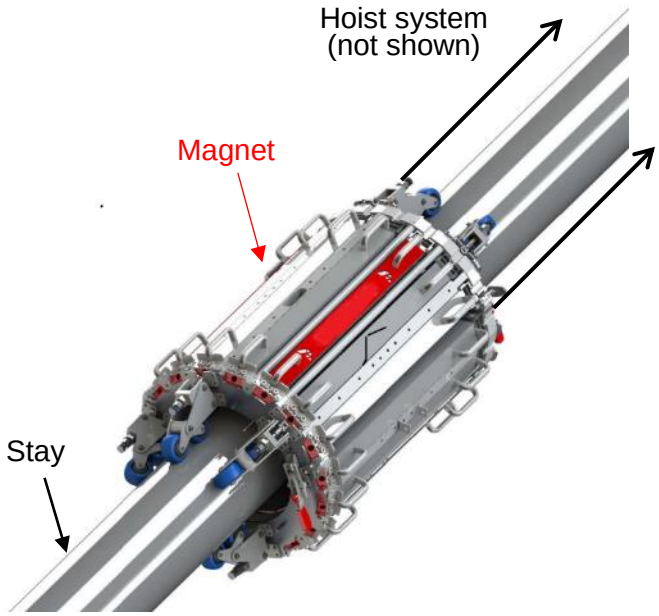

Figure 37 Magnetic testing of cable stays.

As part of the research, we have spoken with most major MFL service providers, including Dywidag (which supplied the strands of the VGCS), Prime NDT Services, Bridge Diagnostics, Inc. (BDI), Bureau Veritas North America, Sixense Monitoring, Structural Monitoring Solutions (SMS), and MISTRAS. We have also spoken with Dr. Hoda Azari, NDE Research Program Manager at FHWA, and Dr. Seung-Kyoung Lee, Former Manager, Coatings and Corrosion Lab at FHWA, who has recently published a comprehensive report on Magnetic Flux-Based Nondestructive Evaluation Technologies [30].

Commercially available MFL magnets are designed for stays up to 14" in diameter, which prevents their applicability to the VGCS stays. The research, communications, and interviews with subject-matter experts indicate the possibility of designing and manufacturing a custom magnet for use in the VGCS. The presence of a stainless-steel sheath does not appear to create any difficulties for the MLF testing, given that the stainless-steel is not a highly magnetic material. Other than the magnet itself, a few critical issues should be considered, including

- A high-capacity hoist system for the heavy magnet required, and
- A cooling system that may be required to dissipate the heat generated during operation.

The conducted studies support the recommendation that MFL should be considered if the inspection results of high-risk areas (e.g., anchorage zones, saddle, and deck level ends of stays) indicate notable concerns with corrosion or other types of deterioration. Given that the MLF primarily inspects the free lengths of the strands, it is important to justify the need to undertake custom-designed MFL testing. Should the inspection of the free lengths of the strands be required, the cost and practicality of pulling (and replacing) a few selected strands and testing them in a laboratory (to determine the extent of the deterioration) should be considered in comparison to the MLF testing.

5. Research Findings and Conclusions

The studies conducted support the following findings and conclusions.

General

- The most critical and prevalent condition causing cable deterioration is the corrosion of the steel strands inside the stays. Other types of deterioration conditions include section loss, breakage or nicking, compromised grout or grease, voids, and water infiltration.
- Stay cables of the Veterans' Glass City Skyway (VGCS) have unique design features to help reduce and delay strand deterioration. These features also make it difficult to inspect the strands using currently available non-destructive evaluation (NDE) methods.
- Literature search, case studies, and subject-matter expert interviews indicate that the deterioration of strands typically starts at the anchorage zones as opposed to the free lengths of the strands. Fortunately, the inspection of anchorage zones is significantly easier for the VGCS than the free lengths of the strands.

Applicable NDE Methods

- The applicable methods for the inspection of the anchorage zones include the removal of anchorage caps and sleeves access at the deck; visual inspection of strand ends, sockets, and locking plates; visual inspection of difficult-access locations such as anchorage boxes and guide pipes using borescopes; and dissection of sheathing for visual inspection of fillers and strands, and material sampling and testing.
- The applicable method for the global health assessment of the cable stays and bridge superstructure includes the vibration-based cable tension estimation methods. These tensions are compared with the baseline tension values that represent healthy conditions.
- The applicable method for the inspection of the free lengths of the strands includes magnetic flux leakage (MFL) testing using a custom-designed magnet. This may also require a high-capacity hoist system to guide the magnet along the stays, and a cooling system to mitigate the effects of the heat generated during the operation.
- Another method for the inspection of the free lengths of the strands includes pulling and replacing a few selected strands and testing them in a laboratory. This was the inspection method envisioned during the design of the VGCS.

Visual Inspection Study

- The visual inspection study conducted using a borescope inspected the lower ends of 14 stays. The inspected strands appeared in very good condition with no signs of strand damage, chipping, or corrosion. The dusty state of the strands implies no water runoff and dry conditions.
- The grease samples collected from the lower ends of the stays appeared in good condition with consistent color, viscosity, and consistency. No concern is detected.
- Eight stays were found with no drain holes, including stays 9B, 10B, 14B, 16B, 17B, 18B, 19B, and 20B. It is recommended that drain holes be added to these stays to match the remaining holes in terms of diameter and location.
- It is recommended that a similar borescope inspection is performed in other high-risk areas, such as the saddle and entrance to the pylon, during future inspection cycles.

Environmental Condition Assessment Study

- The environmental condition assessment study performed using six internal and two external temperature and humidity loggers found no evidence of excessive moisture accumulation inside the stays. The conditions inside the stays are found to be slightly more humid than the ambient (outside) conditions.
- This conclusion is based on the 7.5 months data collected during this study.

The stay force estimation study

- The stay force estimation study conducted using a laser vibrometer on 20 stays found no credible concern for the health of the stay cables of the VGCS. The deviation of

temperature-adjusted stay forces from the lift-off forces measured by the contractor in 2007 is under 10%, which is within the margins of expected deviation.

- It is recommended that a periodical cable tension estimation program be established, with a 4-year measurement cycle, to monitor the global health of the VGCS.
- Tensions of stays 10A-11A-12A and 18B-19B-20B should be measured with close attention in the next measurement cycle. Some of these stays had deviations close to 10%.
- Laser vibrometer measurements from the Robert Craig Memorial Bridge may be considered for future measurements if an extra-long-range lens and proper aiming equipment can be secured. This may eliminate the need to close a lane of the VGCS. In addition, measurements could be split into two nights for a longer duration and multiple rounds of recordings.
- A recording duration of 45 or preferably 60 seconds is recommended for any future measurements.
- For shorter stays (1 to 4), aiming the laser beam to a cheese plate location, where the strand bundle and sheathing may vibrate as a unit, is recommended in the next measurement to assess the influence of this location on the measured frequency.
- Stay forces may be calculated conveniently using Eq. (2) in future measurements. Temperature adjustment should still be applied to these values.

The findings of this study pertain to the inspected areas of the stays and do not imply a comprehensive evaluation of the VGCS. Regular inspection and assessment programs should be continued to monitor the health of the VGCS in the long term.

6. Recommendations for Implementation

The Veterans' Glass City Skyway (VGCS) was opened to traffic in 2007. It is important to have a non-destructive evaluation (NDE) strategy in place to monitor the conditions of the stay cables during the service life of the bridge. This could enable timely remedial actions if or when it becomes necessary. The studies conducted support the feasibility and cost-effectiveness of the following methods for implementation.

- Apply the above-noted NDE methods as a part of a regular inspection program.
- Establish a periodical cable tension estimation program, with a 4-year measurement cycle, to monitor the global health of the VGCS.
- If evidence of notable strand deterioration is detected, consider the evaluation methods for the free lengths of the strands.
  - One option is to design a custom magnet for the magnetic flux leakage testing. This study should also investigate if a custom hoist and a cooling system are necessary.
  - Another option is to pull and replace a few selected strands and test the pulled strands in a laboratory to determine the extent of the deterioration.
  - Both options should be evaluated and compared for their cost, practicality, and reliability before a decision is made, if/when necessary.

7. Bibliography

1. Mehrabi AB. Performance of Cable-Stayed Bridges: Evaluation Methods, Observations, and a Rehabilitation Case. J Perform Constr Facil. 2016;30.

2. Hurlebaus S, Hueste MBD, Karthik MM, Terzioglu T. Inspection Guidelines for Bridge Post-Tensioning and Stay Cable Systems Using NDE Methods [Internet]. Washington, D.C.: Transportation Research Board; 2017. Available from: https://www.nap.edu/catalog/24779

3. Chen WZ, Yang JX. Inspection and Assessment of Stay Cables in Cable Stayed Bridges. Appl Mech Mater [Internet]. 2014;638–640:954–60. Available from: https://www.scientific.net/AMM.638-640.954

4. Griffin RB. Corrosion in Marine Atmospheres. Corros Environ Ind [Internet]. ASM International; 2006. p. 42–60. Available from: https://dl.asminternational.org/books/book/26/chapter/355929/corrosion-in-marine-atmospheres

5. Nürnberger U. Influence of material and processing on stress corrosion cracking of prestressing steel. Mater Corros - Werkstoffe und Korrosion. 1997;48.

6. Li H, Lan CM, Ju Y, Li DS. Experimental and Numerical Study of the Fatigue Properties of Corroded Parallel Wire Cables. J Bridg Eng. 2012;17.

7. Mehrabi AB, Ligozio CA, Ciolko AT, Wyatt ST. Evaluation, Rehabilitation Planning, and Stay-Cable Replacement Design for the Hale Boggs Bridge in Luling, Louisiana. J Bridg Eng [Internet]. 2010;15:364–72. Available from: https://ascelibrary.org/doi/10.1061/%28ASCE%29BE.1943-5592.0000061

8. Onset. HOBO Temperature/RH Data Loggers [Internet]. Available from: https://www.onsetcomp.com/products

9. NWS. National Weather Service [Internet]. Available from: https://www.weather.gov/tbw/dewpoint

10. NWS. National Weather Service.

11. Mehrabi AB, Farhangdoust S. A Laser-Based Noncontact Vibration Technique for Health Monitoring of Structural Cables: Background, Success, and New Developments. Adv Acoust Vib [Internet]. 2018;2018:1–13. Available from: https://www.hindawi.com/journals/aav/2018/8640674/

12. Nazarian E, Ansari F, Azari H. Recursive optimization method for monitoring of tension loss in cables of cable-stayed bridges. J Intell Mater Syst Struct [Internet]. 2016;27:2091–101. Available from: http://journals.sagepub.com/doi/10.1177/1045389X15620043

13. Deng Y, Liu Y, Chen S. Long-Term In-Service Monitoring and Performance Assessment of the Main Cables of Long-Span Suspension Bridges. Sensors [Internet]. 2017;17:1414. Available from: http://www.mdpi.com/1424-8220/17/6/1414

14. Li S, Wei S, Bao Y, Li H. Condition assessment of cables by pattern recognition of

vehicle-induced cable tension ratio. Eng Struct [Internet]. 2018;155:1–15. Available from: https://linkinghub.elsevier.com/retrieve/pii/S014102961630623X

15. Cho S, Yim J, Shin SW, Jung H-J, Yun C-B, Wang ML. Comparative Field Study of Cable Tension Measurement for a Cable-Stayed Bridge. J Bridg Eng [Internet]. 2013;18:748–57. Available from: https://ascelibrary.org/doi/10.1061/%28ASCE%29BE.1943-5592.0000421

16. Duan Y-F, Zhang R, Dong C-Z, Luo Y-Z, Or SW, Zhao Y, et al. Development of Elasto-Magneto-Electric (EME) Sensor for In-Service Cable Force Monitoring. Int J Struct Stab Dyn [Internet]. 2016;16:1640016. Available from: https://www.worldscientific.com/doi/abs/10.1142/S0219455416400162

17. He J, Zhou Z, Jinping O. Optic fiber sensor-based smart bridge cable with functionality of self-sensing. Mech Syst Signal Process [Internet]. 2013;35:84–94. Available from: https://linkinghub.elsevier.com/retrieve/pii/S0888327012003512

18. Haji Agha Mohammad Zarbaf SE, Norouzi M, Allemang RJ, Hunt VJ, Helmicki A, Nims DK. Stay Force Estimation in Cable-Stayed Bridges Using Stochastic Subspace Identification Methods. J Bridg Eng [Internet]. 2017;22. Available from: https://ascelibrary.org/doi/10.1061/%28ASCE%29BE.1943-5592.0001091

19. Fang Z, Wang J. Practical Formula for Cable Tension Estimation by Vibration Method. J Bridg Eng [Internet]. 2012;17:161–4. Available from: https://ascelibrary.org/doi/10.1061/%28ASCE%29BE.1943-5592.0000200

20. Ceballos MA, Prato CA. Determination of the axial force on stay cables accounting for their bending stiffness and rotational end restraints by free vibration tests. J Sound Vib [Internet]. 2008;317:127–41. Available from: https://linkinghub.elsevier.com/retrieve/pii/S0022460X08002095

21. Zui H, Shinke T, Namita Y. Practical Formulas for Estimation of Cable Tension by Vibration Method. J Struct Eng [Internet]. 1996;122:651–6. Available from: https://ascelibrary.org/doi/10.1061/%28ASCE%290733-9445%281996%29122%3A6%28651%29

22. Ren W-X, Chen G, Hu W-H. Empirical formulas to estimate cable tension by cable fundamental frequency. Struct Eng Mech [Internet]. 2005;20:363–80. Available from: http://koreascience.or.kr/journal/view.jsp?kj=KJKHB9&py=2005&vnc=v20n3&sp=363

23. Feng D, Scarangello T, Feng MQ, Ye Q. Cable tension force estimate using novel noncontact vision-based sensor. Measurement [Internet]. 2017;99:44–52. Available from: https://linkinghub.elsevier.com/retrieve/pii/S0263224116307138

24. Kim S-W, Jeon B-G, Cheung J-H, Kim S-D, Park J-B. Stay cable tension estimation using a vision-based monitoring system under various weather conditions. J Civ Struct Heal Monit [Internet]. 2017;7:343–57. Available from: http://link.springer.com/10.1007/s13349-017-0226-7

25. Zarbaf SEHAM, Norouzi M, Allemang RJ, Hunt VJ, Helmicki A, Venkatesh C. Ironton-Russell Bridge: Application of Vibration-Based Cable Tension Estimation. J Struct Eng [Internet]. 2018;144. Available from:

https://ascelibrary.org/doi/10.1061/%28ASCE%29ST.1943-541X.0002054

26. Scott Kangas. Experimental Modeling and Stay Force Estimation of Cable-Stayed Bridges [Internet]. University of Cincinnati; 2009. Available from: https://etd.ohiolink.edu/acprod/odb_etd/etd/r/1501/10?clear=10&p10_accession_num=ucin1258474356

27. Kangas S. Experimental Modeling and Stay Force Estimation of Cable-Stay Bridges. University of Cincinnati, Cincinnati, Ohio; 2009.

28. Lee S-K, Moriya T, Itoi H, Sugawara M, Kanemaru H. Magnetic Flux-Based Nondestructive Evaluation Technologies for Assessing Corrosion Damage in External and Internal Post-Tensioned Tendons : Development Efforts and Evaluation Results [Internet]. Report Num. Federal Highway Administration; 2022. Available from: https://rosap.ntl.bts.gov/view/dot/67626/dot_67626_DS1.pdf

29. Dywidag. Robotics, Inspection and Maintenance [Internet]. Available from: https://dywidag.com/maintenance

30. Lee S-K, Moriya T, Itoi H, Sugawara M, Kanemaru H. Magnetic Flux-Based Nondestructive Evaluation Technologies for Assessing Corrosion Damage in External and Internal Post-Tensioned Tendons : Development Efforts and Evaluation Results. Report Num. Federal Highway Administration; 2022.